Food Bioscience 62 (2024) 105052

Contents lists available at ScienceDirect

Food Bioscience

journal homepage: www.elsevier.com/locate/fbio

Apple vescicles: Revolutionary gut microbiota treatment for Inflammatory Bowel Disease

Letizia Ferroni [a], Andrea Rubini [b], Paolo Bargellini [c], Elena Tremoli [a], Ilenia Pia Cappucci [a], Ugo D'Amora [d], Alfredo Ronca [d], Giulia Calogero [b], Paolo Cortellini Panini [c], Gisella Bettini [e], Cristiana Piccoli [e], Giuseppe Rubini [f], Lucia Sileo [g], Maria Pia Cavaleri [g], Luca Lovatti [g], Barbara Zavan [g,*]

[a] *Maria Cecilia Hospital, GVM Care and Research, Cotignola, 48033, Italy*
[b] *Ultravet Diagnostics, 40017, San Giovanni in Persiceto, Italy*
[c] *Anicura, Tyrus, Terni, Italy*
[d] *Institute of Polymers, Composites and Biomaterials, National Research Council, Naples, 80125, Italy*
[e] *Clinica Veterinaria Estense, Ferrara, Italy*
[f] *ZetaRL, Bologna, Italy*
[g] *Department of Translational Medicine, University of Ferrara, 44121, Ferrara, Italy*

A B S T R A C T

Inflammatory bowel disease (IBD) causes chronic inflammation of the digestive system and can affect both humans and household pets like dogs. Despite extensive research, a definitive cure remains elusive. This study investigates the therapeutic potential of apple-derived extracellular vesicles (ADEVs) in canine IBD. ADEVs, isolated from 'Golden Delicious' apples, were orally administered to dogs with IBD over a ten-day period. Microbiota analysis, clinical assessments, endoscopic examinations, and ultrasound imaging showed a significant reduction in disease severity and post-treatment symptoms. The results indicate that ADEVs regulate intestinal microorganism growth and interact with host cells. In particular IgA and calprotectine level riched physiological level, as well as microbiota and intestinal mucose. These results can explained thanks to the soothing effect of ADEVs on IBD may be due to a synergistic regulatory impact on both intestinal flora and the host's inflammatory response. Overall, these findings suggest a promising new avenue for IBD treatment.

1. Introduction

Inflammatory Bowel Disease (IBD) encompasses a group of chronic digestive tract illnesses characterized by local immune system overactivity, or hypersensitivity (Belkaid & Hand, 2014; Cani et al., 2007; Cani et al., 2008; Clemente et al., 2012; Fontaine et al., 2023; Peterson et al., 2009; The triple burden of malnutrition, 2023; Valdes et al., 2018). These conditions afflict common household pets like cats and dogs, often resulting in severe discomfort, vomiting, diarrhoea, and weight loss, with histopathologic lesions in the stomach, small intestine, or colon in advanced cases (Cai, Wang, & Li, 2021; Glassner et al., 2020; Hashimoto-Hill & Alenghat, 2021; Kopper et al., 2021; Nishida et al., 2018; Takeuchi et al., 2023). Clinical and research studies indicate a multifactorial etiology involving a combination of genetic predisposition and excessive immune responses to enteric species populating the microbiome. IBD leads to the disruption of intestinal homeostasis and alteration in gut microbiota functions, a condition known as dysbiosis (David et al., 2014; Grossberg et al., 2022; Ma et al., 2021; Malewska et al., 2011). Despite significant research efforts, the exact determinants of IBD remain elusive, and a definitive cure is not yet available for human or animal patients (Cai et al., 2021b; Cui et al., 2020; He et al., 2021; Heidari et al., 2021; Shen et al., 2021). Current treatments range from dietary modifications to pharmacotherapy, including the administration of amino salicylates, corticosteroids, and immunomodulators. These treatments aim to alleviate symptoms and vary depending on the severity of the disease (An et al., 2020; Bruno et al., 2021; Liu et al., 2020).

In this context, extracellular vesicles (EVs) are emerging as a novel treatment for canine IBD. EVs are small nanovesicles produced by eukaryotic and prokaryotic organisms as means of cellular communication. They consist of a double lipidic layer incorporating a macromolecular bioactive cargo: proteins, mRNAs, small RNAs, and small molecules (Bokka et al., 2020; Pérez-Bermúdez et al., 2017; You et al., 2021). Vesicles of mammalian origin have already been employed in in

* Corresponding author.
E-mail addresses: lferroni@gvmnet.it (L. Ferroni), barbara.zavan@unife.it (B. Zavan).

https://doi.org/10.1016/j.fbio.2024.105052
Received 8 August 2024; Received in revised form 18 August 2024; Accepted 2 September 2024
Available online 5 September 2024

vitro and in vivo studies to reduce inflammation in cases of IBD (Gao et al., 2022; Kim & Park, 2022; Liu et al., 2022). Plants also produce extracellular vesicles (PDEVs), which have been studied as potential remedies for IBD. For example, turmeric-derived exosomes have been administered orally to murine models, demonstrating soothing and anti-inflammatory properties in inflamed colons. Deng et al. (Deng et al., 2017) found that Brassica oleracea-derived EVs provide protection against ulcerative colitis by targeting dendritic cells, while Man (Man et al., 2021) officinale-derived EVs have been used for targeted drug delivery to the intestine.

Apple-derived extracellular vesicles (ADEVs) have been isolated from the fruit of Malus domestica (Trentini et al., 2022a, 2022b, 2024). Their effects on mammalian cell lines make them promising candidates for anti-inflammatory applications in various immune-related diseases. In this study, we investigated the therapeutic potential of ADEVs in dogs with mild to severe IBD by administering ADEVs orally in liquid form. Our aim was to evaluate the impact of ADEVs on live animals, specifically focusing on IBD symptomatology and the modulation of gut microbiota and inflammatory responses.

2. Results

2.1. ADEVs morphological and nutritional analyses

The ADEVs obtained from 'Golden Delicious' apple fruits were isolated and then characterized dimensionally and morphologically. ADEV dimensions were established by Nanoparticle Tracking Analysis (NTA). Size distribution ranged from 60 to 180 nm with a mean diameter of 123 nm, (Fig. 1A). Transmission Electron Microscopy (TEM) revealed cup-shaped vesicles with a diameter around 100 nm (Fig. 1B), consistent with NTA.

The ADEVs were able to interact with mammalian cells as demonstrated by confocal images were vescicles (red) are present close to the cells (Fig. 1C) were the nucleus in blue and cytoskeletonin green are well defined.

ADEV nutritional content, reported on Table 1 show a content on total fibre 3,6 g/100g, a content of carbohydrates by difference of 10,22 g/100 g, and a content of sugars 9,30 g/100g mainly of fructose and glucose.

The nutritional profile of ADEV, as outlined in Table 1, provides a detailed breakdown of its components. Specifically, ADEV contains a total fiber content of 3.6 g per 100 g of the product. This fiber content contributes to the dietary fiber intake, which is important for digestive health and can aid in various metabolic processes. Regarding carbohydrates, the content is reported to be 10.22 g per 100 g, determined by the difference method, which generally involves subtracting the sum of all other components (such as moisture, protein, fat, and fiber) from the total mass. Of this carbohydrate content, 9.30 g per 100 g are classified as sugars. The sugars in ADEV are primarily composed of simple sugars, notably fructose and glucose. These sugars are easily digestible and can

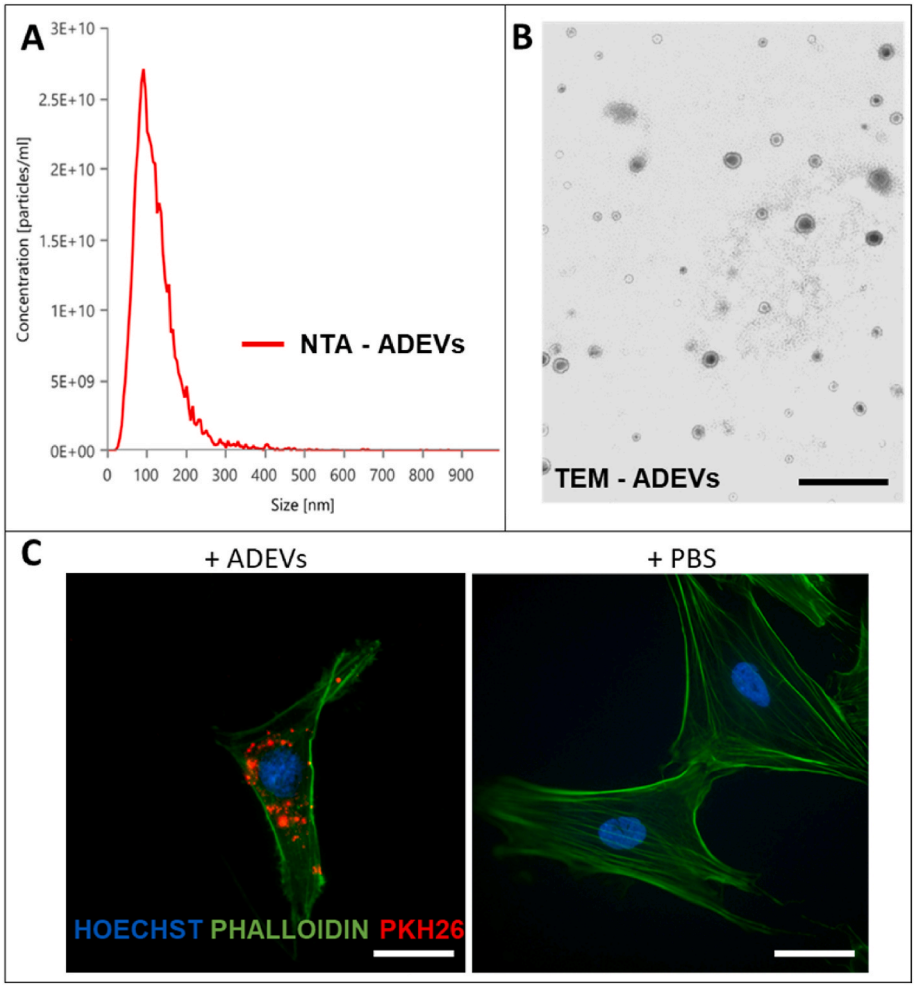

Fig. 1. ADEVs characterization. **A**) Particle size distribution of ADEVs evaluated by NTA. **B**) Representative TEM image of ADEVs with a diameter around 100 nm and cup shape morphology. Magnification: 200,000x. **C**) Representative fluorescence image of ADEVs internalized in cASCs. PKH26-stained ADEVs (red) are uptaken by cells, whose actin filaments (green) are stained with AlexaFluor-488 phalloidin, and nuclei are labeled in blue with Hoechst DNA-specific stain. Scale bar: 50 μm. (For interpretation of the references to color in this figure legend, the reader is referred to the Web version of this article.)

Table 1
Nutritional values of ADEVs.

Parameter	Measure Unit	ADEVs
Moisture	g/100 g	85.28
Ash	g/100 g	<0.25
Total nitrogenous substances, protein (by calculation)	g/100 g	<0.96
Total fat substances	g/100 g	<0.25
Total dietary fibre	g/100 g	3.26
Carbohydrates by difference	g/100 g	10.22
Kcal	g/100 g	53.00
Kj	g/100 g	221.00
Salt (as NaCl)	%	<0.25
SUGARS:		
Fructose	g/100 g	6.50
Glucose	g/100 g	2.50
Lactose	g/100 g	N.A.
Maltose	g/100 g	0.30
Sucrose	g/100 g	N.A.
Total sugars	g/100 g	9.30

quickly impact blood sugar levels. The predominance of these simple sugars indicates that a significant portion of the carbohydrate content is derived from sugars rather than complex carbohydrates or starches. In summary, while ADEV provides a decent amount of dietary fiber, the high sugar content, mainly consisting of fructose and glucose, may be a point of consideration for individuals monitoring their sugar intake. The overall nutritional content underscores the need to balance the consumption of such products with other dietary components to maintain a well-rounded and health-conscious diet.

2.2. Clinical evaluation of IBD symptoms and severity

The presence of chronic gastrointestinal symptoms was defined through the observation of the most common clinical signs: vomiting, diarrhoea, mucoid faeces, hematochezia, and melena. Before the 10-day treatment with ADEVs, all dogs showed the presence of at least one of the above-mentioned signs, after treatment a greater than 50% reduction was observed for each symptom and 69% of treated dogs showed absence of symptoms (Fig. 2 left panel). In particular, mucoid faeces, vomiting and diarrhoea were decreased at 12%, followed by watery diarrhoea alone (4%), vomiting alone (2%), hematochezia (1%), and melena (0%).

The severity of IBD was assessed by the Clinical Inflammatory Bowel Disease Activity Index (CIBDAI) (Fig. 2 right panel). Before the 10-day treatment, IBD cases were mostly moderate (65%), followed by mild (25%) and severe (10%). After treatment, half of the dogs recovered while the other half showed a 50 percent reduction in severity level.

The definition of IBD status determined also by means of the utilization of endoscopic and ultrasound technologies. The detailed

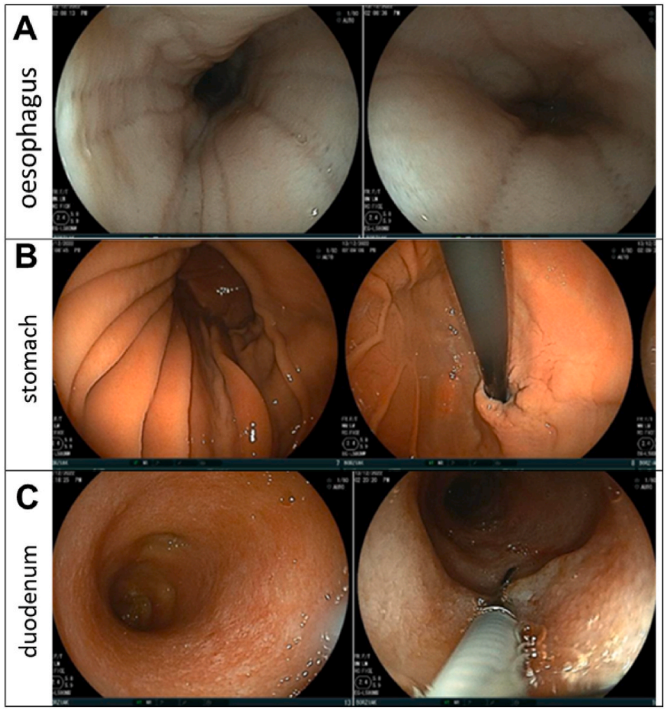

Fig. 3. Representative endoscopic images of A) esophagus, B) stomach and C) duodenum in dogs with IBD after the ten-day treatment with ADEVs.

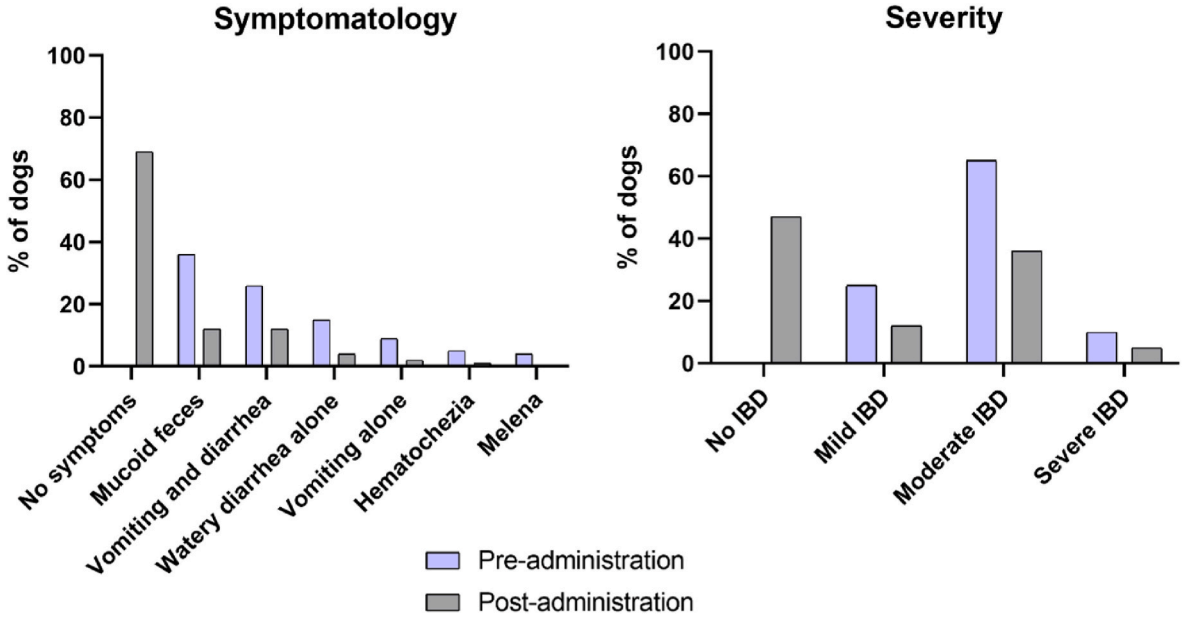

Fig. 2. IBD symptomatology and severity in dogs before and after the ten-day administration period of ADEVs. The left panel shows the percentage of dogs exhibiting diverse symptoms, while the right panel shows the percentage of dogs with no, mild, moderate, or severe IBD. The severity of IBD in each dog has been evaluated by CIBDAI score.

endoscopic findings for the stomach, duodenum, ileum, and colon are extensively documented in Fig. 3A–C. A thorough macroscopic examination of the esophagus and lower esophageal sphincter across all study dogs revealed no abnormal findings, indicating normal anatomical and functional characteristics in these areas.

The predominant endoscopic observations included significant mucosal erythema and increased friability in several regions of the gastrointestinal tract. In the esophagus (Fig. 3A), the examination demonstrated that the organ was normally distensible, maintaining a regular caliber throughout its length. The mucosal surface of the esophagus was observed to be rose-colored, smooth, and shiny. Notably, diffuse brownish pigmentation was present, which is consistent with the age of the patient and may reflect age-related changes. The cardia, located on the esophageal side, was noted to be physiologically closed, which is an expected finding.

In the stomach (Fig. 3B), it was observed to be normally distensible, with no unusual restrictions noted. The mucosal layer was diffusely moderately hyperaemic, indicating a general reddening of the mucosa due to increased blood flow. Additionally, the mucosa exhibited signs of edema, characterized by swelling and fluid retention. The pyloric antrum showed areas of discoloration, which may suggest localized changes or damage. The pylorus itself presented a hypertrophic fold; despite this, it was still passable by the endoscopic instrument. The mucosal surface in both the antrum and pylorus displayed areas of diffuse superficial erosion, indicative of surface-level damage that could be due to irritation or other pathological processes.

In the duodenum (Fig. 3C), the organ was found to be normally non-inflatable, maintaining a consistent caliber throughout the examined segment. The duodenal mucosa was observed to be diffusely severely hyperaemic and moderately edematous. This severe reddening and swelling suggest significant inflammatory changes. The villi, which are small, finger-like projections on the mucosal surface, appeared subjectively thickened and had a clubbed appearance, possibly due to inflammation or other pathological changes. Furthermore, Peyer's patches, which are clusters of lymphoid tissue that play a role in immune surveillance, were prominently visible, indicating normal immune activity within the duodenal mucosa.

Overall, these endoscopic findings provide a detailed view of the gastrointestinal tract's condition, highlighting specific areas of mucosal erythema, edema, and erosion. These observations are crucial for understanding the extent of inflammation and damage in the gastrointestinal tract of the study subjects.

The determination of IBD status was further refined using advanced ultrasound technologies, which provided detailed visualization of the affected areas. As shown in Fig. 4A, ultrasound imaging revealed significant signs of intestinal inflammation. The images displayed a markedly thickened and hypoechoic intestinal wall, a common indicator of inflammation, highlighted by the yellow circle. This thickening of the intestinal wall is a hallmark of IBD, reflecting the infiltration of inflammatory cells and edema. The hypoechoic nature of the wall suggests a high level of fluid and inflammatory cell accumulation, which is typical in inflamed tissues. In addition to these changes in the intestinal wall, the ultrasound also detected multiple inflamed and enlarged lymph nodes located within the submucosal layer, as indicated by the red circles. These lymph nodes appeared enlarged and more hypoechoic than normal, indicating a reactive or inflammatory state. The presence of such lymphadenopathy is frequently associated with chronic inflammation and immune responses in the gut, further confirming the diagnosis of IBD. By contrast, following a treatment period with ADEVs, there was a significant improvement in the ultrasound appearance of the intestinal mucosa. As depicted in Fig. 4B, the previously thickened and hypoechoic intestinal wall showed a more refined and normalized appearance, indicating a reduction in inflammation. The wall thickness was notably reduced, returning towards normal levels, which suggests that the inflammatory process had subsided considerably. The echogenicity of the wall also improved, reflecting a decrease in fluid content

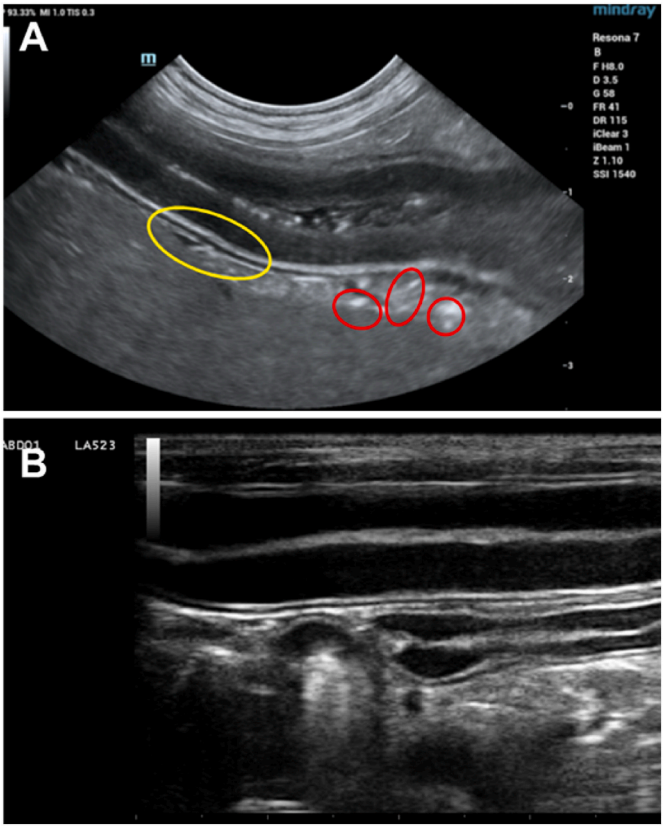

Fig. 4. Abdomen ultrasound imaging in dogs with IBD, A) before and B) after administration of a ten-day treatment with ADEVs.

and inflammatory cell infiltration. Moreover, the size and number of inflamed lymph nodes within the submucosal tissue were markedly reduced. In Fig. 4B, these lymph nodes appeared smaller and less hypoechoic, indicating a resolution of the inflammatory response. This reduction in lymph node inflammation further supports the efficacy of ADEVs in ameliorating the inflammatory response associated with IBD. The observed changes in the ultrasound images underscore the potential of ADEVs as a therapeutic agent, offering a novel approach to reducing intestinal inflammation and associated symptoms in canine IBD. The improvements in both the intestinal wall and lymph nodes highlight the comprehensive anti-inflammatory effects of ADEVs, making them a promising candidate for future therapeutic strategies.

2.3. *Canine microbiota*

Canine microbiota has been evalutated before and after the treatment with ADEVs in order to precisely identify and quantify specific probiotic species, such as Faecalibacterium prausnitzii, Clostridium hiranonis, as well as bacterial genera such as Blautia and Fusobacterium (Fig. 5). These species are critical indicators of gut health and are known for their anti-inflammatory properties and roles in maintaining intestinal homeostasis. Following the administration of ADEVs in dogs diagnosed with IBD, a statistically significant increase in the concentrations of Fusobacterium sp. and Blautia sp. was observed. These concentrations exceeded the established threshold of 1.0E+06 CFU/g, which is indicative of a healthy gut microbiota in canines. This suggests that ADEVs have a positive impact on enhancing the populations of these beneficial microbial species. Although there was an observed increase in the concentrations of F. prausnitzii and C. hiranonis post-treatment, these changes did not achieve statistical significance, indicating that while there was a positive trend, the variation was not sufficient to confirm a consistent effect across all subjects. In addition to monitoring probiotic

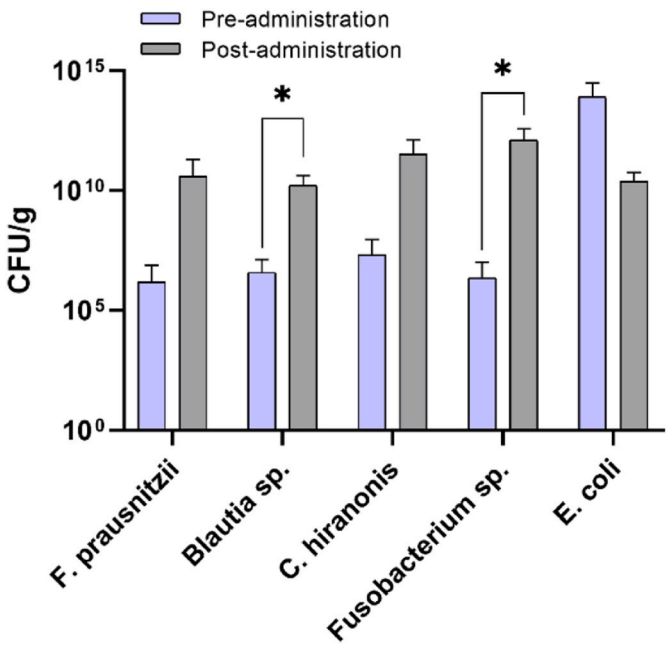

Fig. 5. Canine microbiota analyses performed before and after the ten-day treatment with ADEVs: quantification of *F. prausnitzii*, *Blautia* sp., *C. hiranonis*, *Fusobacterium* sp. and *E. coli* by PCR. Statistical analysis p-values: *<0.01, **<0.001, ***<0.0001.

species, the study also focused on quantifying the opportunistic pathogen Escherichia coli (E. coli) in the stool samples. E. coli is known for its involvement in the etiopathogenesis of IBD, with certain pathotypes exacerbating the inflammatory response in the gut (Fig. 5). Post-treatment results indicated a substantial reduction in the concentration of E. coli, decreasing from 7.9E+13 CFU/g to 2.4E+10 CFU/g. Despite this significant decrease, the E. coli levels remained above the typical concentration range observed in healthy dogs, which spans from 1.0E+06 to 1.0E+09 CFU/g. This suggests that while ADEVs effectively reduce the load of pathogenic E. coli, further intervention may be required to bring these levels down to those comparable with healthy canine microbiota. The observed changes in the microbial populations highlight the potential of ADEVs as a therapeutic agent in managing IBD in dogs. The significant increase in beneficial microbial species such as Fusobacterium and Blautia and the concurrent reduction in pathogenic E. coli indicate a shift towards a more balanced and health-promoting gut microbiota. This microbial modulation is likely contributing to the overall anti-inflammatory effects observed in the treated dogs, providing a promising avenue for further research and development in veterinary medicine for the treatment of IBD.

2.4. Biochemical parameters

Among the biomarkers indicative of bowel inflammation, secretory immunoglobulin A (sIgA) and calprotectin (CALPRO) were quantified in fecal samples using the enzyme-linked immunosorbent assay (ELISA) methodology. Both of these markers are crucial in assessing intestinal mucosal immune responses and inflammatory states. Quantitative analysis revealed a significant decrease in the levels of sIgA and CALPRO following treatment with ADEVs. Specifically, the concentration of sIgA in the fecal samples was reduced to 1.80 mg/g, which is notably lower than the upper reference threshold of 3.21 mg/g typically observed in fecal matter from healthy canines. This substantial reduction in sIgA levels indicates a potential normalization of mucosal immune activity and a decrease in inflammatory responses within the gut.

Similarly, calprotectin levels also showed a marked decrease, falling to 38.20 μg/mL. This reduction is below the maximal threshold of 41 μg/mL that is commonly associated with healthy fecal samples. Calprotectin is a well-established marker of intestinal inflammation, and its decreased concentration further supports the effectiveness of ADEVs in reducing inflammatory processes in the gastrointestinal tract. These results collectively suggest that ADEVs have a significant impact on modulating intestinal inflammation, as evidenced by the reduction in both sIgA and CALPRO levels. The decrease in these biomarkers reflects a potential therapeutic benefit of ADEVs in restoring mucosal homeostasis and alleviating inflammatory conditions in the gut. This promising outcome underscores the need for further investigation into the mechanistic pathways through which ADEVs exert their anti-inflammatory effects and their potential for broader application in managing inflammatory bowel diseases in veterinary practice.

3. Discussion

Inflammatory Bowel Disease (IBD) is characterized by intestinal dysbiosis and heightened local immune activity (Ye et al., 2023). Although a definitive cure remains elusive, therapies such as dietary modifications and pharmacological interventions can mitigate symptoms. Additionally, manipulating the gut microbiota with probiotics and prebiotics is a recognized strategy for symptom relief in IBD (Suchodolski et al., 2012). An optimal therapeutic approach for IBD should target both the regulation of microbial populations and the modulation of the host immune response. Extracellular vesicles (EVs) play a significant role in cellular communication and have been widely studied in inflammatory diseases, including IBD (Rhimi et al., 2022). This study explores the impact of apple-derived extracellular vesicles (ADEVs) on the gut microbiota and gastrointestinal mucosa of dogs suffering from IBD, utilizing microbial quantification, endoscopic and ultrasound analyses, and symptom evaluation.

Apple EVs, isolated using a previously established method, exhibited the typical morphology and size distribution of plant EVs. Their interaction with mammalian cells, previously demonstrated in studies, was corroborated in our examinations using canine cell lines (Fig. 1).

The effect of ADEVs on gut microbiota was assessed in vivo. This investigation aimed to evaluate the potential of ADEVs as a treatment for dysbiosis-related pathologies. For this purpose, medium-sized companion dogs with IBD were selected as model subjects. IBD is a common cause of chronic gastrointestinal symptoms in dogs, stemming from an abnormal immune response often triggered by an exaggerated reaction to non-pathogenic gut bacteria (Díaz-Regañón et al., 2023). Following a ten-day regimen of daily ADEV administration, comprehensive clinical assessments were conducted in accordance with established guidelines. The data collected indicated a significant reduction in disease severity, symptom manifestation, and intestinal inflammation post-treatment (Figs. 3 and 4).

The improved health status of the treated dogs can be attributed to two primary aspects of ADEVs' biological activity: their influence on microbial growth and their immunomodulatory effects (Fig. 5). Fecal analysis post-treatment revealed changes in the microbial population, including an increase in Blautia sp. and Fusobacterium sp., both associated with IBD progression. Blautia species, part of the Lachnospiraceae family within the Firmicutes phylum, are abundant in mammalian gut microbiota and play a crucial role in mucus production in the colon, which is often compromised in IBD. Reduced Blautia levels have been linked to dysbiosis and related diseases, as these bacteria metabolize carbohydrates to produce anti-inflammatory metabolites such as acetate. Although Fusobacterium spp. are known pathogens in humans, they are prevalent in healthy canine microbiota, and their reduction is associated with IBD-related dysbiosis. This distinction underscores the differences in IBD etiology between humans and dogs (Mayer, 2000; Vázquez-Baeza et al., 2016). Our findings suggest that ADEVs promote the presence of species associated with a healthy gut microbiota in dogs, indicating potential benefits for dysbiosis-related conditions. However, further research on ADEV effects on human microbiota is warranted.

Regarding the immunomodulatory effects of ADEVs, our results indicate a reduction in inflammatory markers sIgA and fecal CALPRO in treated dogs (Fig. 6) (Pathirana et al., 2018). ADEVs have demonstrated anti-inflammatory properties in human cell studies, making them promising candidates for treating inflammatory conditions. Literature suggests that EVs can traverse the intestinal barrier and deliver intact molecular messages to the intestine. For example, milk-derived EVs administered orally can withstand gastrointestinal conditions and enhance intestinal barrier integrity. The current study shows ADEVs' ability to interact with and permeate canine cells, as evidenced in Fig. 1C. By being absorbed into the cells, ADEVs may initiate molecular signaling pathways or modulate cellular processes that contribute to symptom alleviation in treated dogs.

4. Conclusions

In summary, this study elucidates the therapeutic efficacy of apple-derived extracellular vesicles (ADEVs) in treating canine inflammatory bowel disease (IBD), with a specific focus on nutritional modulation and gut microbiota balance. Through extensive in vitro and in vivo analyses, our research demonstrated that ADEVs effectively suppress the proliferation of pathogenic gut microorganisms while fostering the growth of beneficial probiotic species, thereby promoting a healthier intestinal environment.

The administration of ADEVs over a ten-day period resulted in significant clinical improvements in dogs suffering from IBD. Notably, these improvements included enhanced integrity of the mucosal layer, reduced inflammation of lymph nodes, and decreased levels of inflammatory biomarkers in faeces. The ability of ADEVs to promote a favorable microbiota composition is of particular interest, as a balanced gut microbiota is crucial for maintaining overall health and managing chronic gastrointestinal conditions like IBD. Nutritionally, ADEVs represent a novel approach to modulating the gut environment. The vesicles contain bioactive compounds that may influence microbial populations and host immune responses. The dietary inclusion of such bioactive molecules has the potential to restore microbial equilibrium, which is often disrupted in IBD. By fostering the growth of commensal bacteria such as Blautia and Fusobacterium species, ADEVs contribute to the production of short-chain fatty acids and other metabolites that support mucosal health and anti-inflammatory processes. These probiotic bacteria play a crucial role in the fermentation of dietary fibers, producing metabolites that reinforce the intestinal barrier and modulate immune function. The study also highlighted the systemic effects of ADEVs, demonstrating their capacity to traverse the gastrointestinal tract and exert their biological activities at various sites. This systemic action underscores the potential of ADEVs to not only target local gut inflammation but also to modulate systemic immune responses, which is essential in the comprehensive management of IBD.

In conclusion, the findings from this study underscore the potential of ADEVs as a promising therapeutic modality for canine IBD. Their dual role in modulating gut microbiota and exerting immunomodulatory effects positions them as a unique nutritional intervention. Further research is warranted to fully elucidate the mechanisms through which ADEVs exert their beneficial effects and to explore their broader clinical applicability in veterinary medicine. Future studies should also consider the long-term impacts of ADEV administration on gut health and overall nutritional status, as well as potential synergistic effects with other dietary interventions aimed at managing IBD in canines.

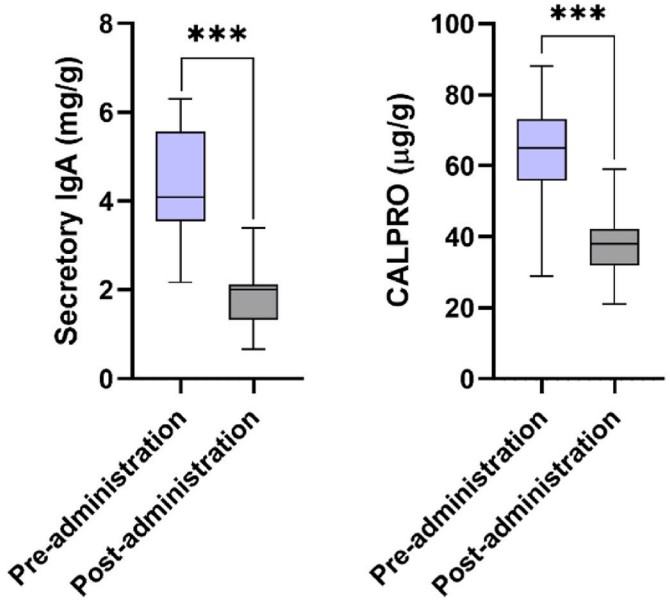

Fig. 6. Quantification of sIgA (left panel) and CALPRO (right panel) by ELISA. Statistical analysis p-values: *<0.01, **<0.001, ***<0.0001.

5. Methods

5.1. ADEVs isolation

ADEVs were isolated from DOP 'Golden Delicious' variety apple cultivar fruit (*Malus domestica*) sourced from Val Di Non (Trentino, IT) following the protocol outlined in previous works [35]. The obtained pellet was resuspended in 1 mL of Phosphate Saline Buffer (PBS; Thermo Fisher Scientific, MA, USA) pH 7.4, aliquoted and stored at −80 °C until further use.

5.2. Nanoparticle Tracking Analysis (NTA)

NTA uses light scattering to determine the concentration of particles in suspension and determine their diameter by following their Brownian motions. The measurement was performed with the instrument NanosightPro (Malvern Panalytical, Worcestershire, UK). Each ADEVs sample was diluted in 1 mL of PBS to obtain optimal concentrations for detection (between 1E+06 and 1E+09 particles/mL). The sample flowed at a 3 μL/min speed through a chamber lighted with a laser beam, and a camera recorded the scattered light. Five recordings of 5 min were processed by Nanosight's software, which tracks individual particles and their movement in the suspension. The concentration and particle size were calculated by taking into account the temperature, viscosity and dilution of the sample. Data is represented as particle concentration (particles/mL) for particle size distribution (nm).

5.3. Transmission Electron Microscopy (TEM)

TEM imaging was conducted on the ADEVs fraction following the method of Corona et al. [60]. Briefly, a concentration of 1E+09 particles/mL was applied to a TEM Grid 200 Mesh Cu/Pd. Fixation was performed using a solution containing 2% paraformaldehyde and 1% glutaraldehyde in 100 mM PBS at pH 7.4. Staining was performed using a contrasting solution of Methylcellulose/Uranyl Acetate for 10 min. The grid was subsequently dried, and images were captured using a TEM Zeiss EM 910 instrument (Carl Zeiss Microscopy, Oberkochen, Baden-Württemberg, Germany) equipped with a CCD digital camera (Ultrascan 1000, Gatan, Munich, Germany).

5.4. ADEVs uptake in canine adipose-derived stem cells

Canine adipose-derived stem cells (cASCs) were isolated from the fat tissue of canine specimens, as previously described [22]. Briefly, biopsies of adipose tissue were sliced and digested for 3 h at room temperature (RT), with a solution of collagenase type II (Sigma-Aldrich, MO, USA) in Hanks' Balanced Salt Solution (HBSS) with calcium and magnesium

(EuroClone, Milan, IT). After the digestion, cASCs were incubated in Dulbecco's Modified Eagle's Medium-high glucose (Sigma-Aldrich) supplemented with 2% antibiotic antimycotic (Sigma-Aldrich) and 10% Foetal Bovine Serum (FBS) (Thermo Fisher Scientific) at 37 °C and 5% CO_2.

ADEVs (1E+09 particles/mL) were stained with PKH26 Red Fluorescent Cell Linked Midi Kit for General Cell Membrane Labelling (Sigma-Aldrich). EVs were stained by a 5-min incubation with PKH26 dye in the diluent solution (Diluent C). The staining was blocked by adding an equal volume of a 2% BSA solution. To re-pellet stained ADEVs, the volume was brought to 20 mL with PBS, and it was centrifuged at 110.000 rcf for 1 h in Ultracentrifuge Optima L-70 and rotor type 70 Ti (Beckman Coulter Inc.). The supernatant was removed, and the pellet of stained ADEVs was resuspended in 200 μL of PBS. For staining, cASCs were seeded on 13 mm cover slides, and then treated with 50 μL of PKH26-labeled ADEVs for 6 h. Cells were then washed thoroughly with PBS and fixed with a solution of 4% paraformaldehyde in PBS for 15 min at RT. Afterwards, slides were incubated in 2% BSA for 30 min, rinsed again with PBS, stained sequentially with AlexaFluor™ 488 Phalloidin (Sigma-Aldrich) and fluorescent dye Hoechst (Sigma-Aldrich) to label actin and nuclei, respectively. Images were acquired with a Nikon Eclipse Ti Fluorescence Microscope (Nikon, Tokyo, JPN) equipped with a 60x oil objective.

5.5. Nutritional analyses

The ISTISAN Reports 1996/34 from Italy's Istituto Superiore di Sanità present thorough guidelines for evaluating crucial nutritional components in food, such as moisture, ash, fat, and sodium chloride (salt) content. The process for moisture determination begins with the sample undergoing an initial evaporation step using a boiling water bath to remove most of the liquid. Following this, the sample is transferred into a capsule and placed in an oven manufactured by Memmert GmbH (Nürnberg, Bavaria, Germany) set to 130 °C. The capsule, containing a 10 mL sample, is then heated at 500 °C for 5 h. Once the heating is complete, the capsule is cooled in a vacuum desiccator (ThermoFisher Scientific) for 1 h, after which it is weighed. The moisture content is calculated based on this final weight, using the specified formula.

$$\text{Moisture (g/100g)} = (E\text{-}m) \times 100/E$$

Where "E" is the initial mass of the sample in grams, and "m" is the mass of the dry sample.

To determine the ash content, 20 mL of the liquid sample is transferred into a tared capsule. This capsule is placed in a boiling water bath until all the water has evaporated. The ash content is then determined by weighing the residue and using the formula:

$$\text{Ash (g/100g)} = (M1/M0) \times 100$$

Where "M1" is the mass of the sample aliquot, and "M0" is the mass of the residue.

The lipid component of the sample is extracted by performing acid hydrolysis. A 50 mL sample is heated at 80 °C for 1 h with 3N hydrochloric acid (HCl) to break down the material. After digestion, the solution is cooled and passed through a double layer of filter paper by gravity. The filtered residue is rinsed and then dried in a vacuum oven set at 75 °C for 1.5 h. Once drying is complete, the filter is transferred to an extraction apparatus, where 50 mL of petroleum ether is used to extract the lipids. The solvent is evaporated, and the remaining residue is dried again in the vacuum oven before being weighed. The total fat content is then calculated using the relevant formula.

$$\text{Total Fat (g/100g)} = (A\text{-}B)/C \times 100$$

Where "A" is the weight of the flask containing the extracted fat, "B" is the weight of the tared flask, and "C" is the weight of the sample used for the analysis.

Sodium chloride (NaCl) is quantified through a gravimetric titration method, starting with the sample's ashes. To begin, 5 mg of the ashes are combined with 100 mL of water and 10 mL of 0.1 N silver nitrate (AgNO3). Next, 15 mL of concentrated nitric acid (HNO3) is introduced into the mixture. The solution is then brought to a boil for 10 min with constant stirring and subsequently allowed to cool to room temperature. After cooling, the excess AgNO3 is titrated using 0.1 N ammonium sulphocyanide in the presence of a ferric alum solution that has been acidified with nitric acid. The NaCl concentration is then determined using a specific calculation formula

$$Cl_{tot} = (10 - mL1) \times PM_{Cl} \times 2.5E\text{-}4$$

$$\text{NaCl tot} = (10 - mL1) \times PM_{NaC} \times 2.5E\text{-}4$$

Where mL1 corresponds to the mL of solution of ammonium sulphocyanate consumed in the titration; $PM_{Cl} = 35.45$; $PM_{NaCl} = 58.44$.

Total protein content is quantified according to ISO 1871:2009, which utilizes the Kjeldahl digestion method to measure nitrogen levels, subsequently converting them into protein content. Total dietary fiber is determined using the AACC International Approved Method 32–45.01 (AOAC method 2009.01), which involves enzymatic digestion to replicate the human digestive process, allowing for the accurate measurement of fiber content.

To calculate the total carbohydrate content, the values for protein, fat, and dietary fiber are subtracted from the sample's overall weight. The caloric content, expressed in kilocalories (Kcal) and kilojoules (KJ), is derived using the conversion factors outlined in Directive 90/496/EEC, based on the nutritional data obtained from the samples.

For the quantification of specific sugars—fructose, glucose, lactose, maltose, and sucrose—two solutions were prepared: i) Carrez Solution 1 was prepared by dissolving 119 g of zinc acetate dihydrate and 15 g of glacial acetic acid in deionized water to make 500 mL; ii) Carrez Solution 2 involved dissolving 53 g of potassium ferrocyanide in 500 mL of deionized water. The sample preparation process included adding 5 mL each of Carrez Solution 1 and Carrez Solution 2–50 mL of the sample, which was then diluted to 100 mL with deionized water. The sugars were measured using ion chromatography, with 150 mM sodium hydroxide as the eluent at a flow rate of 1 mL/min. Detection was carried out using a pulsed amperometric detector (Antec Scientific, NL), and the sample concentrations were compared to those of standard sugar solutions. The quantities are reported as g/100 g, calculated using the appropriate formula:

$$\text{Sugars} = (AxC)/B \times F \times (100/ML)$$

Where A is the area of the sugar peak, C is the concentration (mg/mL) of the standard solution for each sugar, B is the area of the peak of the sugar in the standard solution, F is the dilution factor of the sample, ML is the volume of samples used for the analysis.

5.6. Dog enrolment and sample harvesting

Dogs were selected according to the World Small Animal Veterinary Association (WSAVA) (30) guidelines for diagnosing idiopathic IBD, which include: i) Presence of chronic gastrointestinal symptoms lasting more than three weeks, such as anorexia, vomiting, weight loss, diarrhoea, hematochezia, or mucoid faeces; ii) histopathological evidence of mucosal inflammation; iii) exclusion of other potential causes of gastroenterocolitis through comprehensive diagnostic evaluation; iv) lack of adequate response to properly administered therapeutic interventions, including dietary changes, antibacterial treatments, and deworming medications; v) positive clinical response to anti-inflammatory or immunosuppressive medications (Inflammatory Bowel Disease Fact Sheet; Jergens et al., 2003).

The severity of IBD in dogs was assessed using the Clinical Inflammatory Bowel Disease Activity Index (CIBDAI) developed by Jergens

et al. [46]. Dogs were categorised based on their CIBDAI scores as having mild IBD (score 4–5), moderate IBD (score 6–8), or severe IBD (score >9). The study comprised 87 dogs (41 males and 46 females) suffering from chronic gastrointestinal issues, aged from 1 to 10 years (median age: 5.5) representing various breeds including non-descript, German Shepherds, Labradors, Golden Retriever, Pincer, Rottweiler, Boxer, Lhasa Apso.

Every day for 10 days, 1 mL of ADEVs concentrate 6E+08 particles/mL was administered orally to the dogs. It is crucial that the administration occurs with the stomach empty, meaning that the treatment should be given at least 2 h away from any meals. This ensures that the physiological absorption and interaction of the administered proteins are not affected by the presence of food in the gastrointestinal tract. The choice of a 10-day administration period was based on our understanding of the time required for therapeutic interventions to produce observable clinical effects. Specifically, this duration aligns with the minimum timeframe necessary to assess the cessation of diarrhoea, which is a key endpoint in evaluating the efficacy of the treatment. This period was determined through both preliminary studies and a review of relevant literature, which suggest that 10 days is sufficient for the administered exosome-derived proteins to interact with the gastrointestinal system, facilitate any physiological changes, and lead to the resolution of diarrhoea. The extended duration ensures that the treatment has adequate time to exert its effects, allowing for the observation of any significant improvements in gastrointestinal health and symptom relief. This approach aims to standardize the intervention period and provide a reliable assessment of the treatment's efficacy in ameliorating gastrointestinal symptoms.

Faecal tests involve analysing a fresh stool sample within 24 h. Each stool sample was divided into three parts and frozen at − 80 °C for 72 h before analysis of inflammation markers by ELISA and microbiota analysis by Copro PCR.

5.7. Immunoglobulin A (sIgA) and calprotectin

Secretory immunoglobulin A (sIgA) and canine calprotectin (CALPRO) present inside the faeces of the dogs were quantified with Dog Secretory Immunoglobulin A (sIgA) ELISA Kit (Abbexa, Cambridge, UK) and Dog Calprotectin ELISA Kit (Abbexa), respectively. All stool specimens were diluted at a ratio of 1:11 with a diluent solution and mixed thoroughly to achieve emulsification. The mixture was allowed to stand at room temperature for 30 min to facilitate the precipitation of particles, after which the clear liquid (supernatant) was collected. The ELISA assays were performed following the manufacturer's guidelines. In summary, 100 μL of each standard and sample were added to the wells of a microplate and incubated at 37 °C for 1 h. After removing the liquid, 100 μL of Detection Reagent A was introduced to each well and incubated for an additional hour at 37 °C. Subsequently, the solution was replaced with 100 μL of Detection Reagent B working solution and incubated at 37 °C for 30 min. The final step involved adding 90 μL of TMB Substrate to each well, with incubation at 37 °C for 20 min in the dark. Following this, 50 μL of Stop Solution was added to each well, and the absorbance was measured immediately at 450 nm (Abs450) using the Victor3 multi-plate reader (Perkins). To determine CALPRO and sIgA concentrations, the Abs450 values for each standard and sample were adjusted by subtracting the Abs450 of the blank sample. The corrected Abs450 values for each standard were plotted against their respective concentrations, and the sample concentrations were then estimated from the standard curve.

5.8. Microbioma analyses

Microbial DNA was extracted from 0.2 g of faecal samples with PureLink™ Microbiome DNA Purification Kit (Invitrogen), following the manufacturer's instructions. The PCR was performed on the isolated DNA samples to detect and quantify M.O. species such as *F. prausnitzii*, *Blautia* sp., *C. hiranonis*, *Fusobacterium* sp. and *E. coli*. *Fusobacterium* sp. was detected with AffiVET® Fusobacterium sp. PCR kit (Affigen, TX, USA), while *F. prausnitzii*, *Blautia* sp. and *E. coli* with COLONOFLOR PCR kit (AlphaLab, Saint-Petersburg, RU).

5.9. Endoscopic assessment

Endoscopic procedures encompassing gastroduodenoscopy and colonoscopy were conducted using N. 60914 PKS Veterinary Video endoscope (Karl Storz, DE). This advanced endoscope boasted an outer diameter of 9.8 mm, a biopsy channel diameter of 2.8 mm, and a working length of 1400 mm. Biopsy samples were meticulously obtained using specialized fenestrated long oval cup biopsy forceps of 2.2 mm diameter (Karl Storz). To ensure comprehensive documentation, digital images of the endoscopic findings were systematically captured.

Before the procedure, stringent preparatory measures were adhered to, to mitigate potential risks. Animals were subjected to a fasting period lasting 24–48 h, with water intake restricted for 4 h preceding the examination. Additionally, oral laxatives were administered the day prior, coupled with an electrolyte-based enema administered pre-procedure. The endoscopic examination was conducted with the dog positioned in left lateral recumbency under general anaesthesia, following established protocols. Throughout the gastroscopy, any discernible lesions were documented and evaluated using a standardized report form endorsed by the WSAVA Gastrointestinal Standardization Group for upper and lower gastrointestinal endoscopy. Furthermore, four to five representative biopsy samples were judiciously collected using punch biopsy forceps. Mucosal abnormalities spanning hyperaemia, edema, discolouration, granularity, haemorrhage, erosions, and ulcers were scrutinized across the gastrointestinal tract. Utilizing a comprehensive scoring system ranging from 0 to 3, the presence and extent of these aberrations were meticulously quantified. Subsequently, a composite score was derived by summing the points obtained from each segment of the gastrointestinal tract.

5.10. Statistical analysis

All values are expressed as mean ± standard error (SE). The difference between three or more groups was determined by one-way ANOVA, followed by the Bonferroni post hoc test, while a paired parametric *t*-test was performed between two groups on samples referring to before and after treatment (GraphPad Software). Statistical difference is expressed as p-value and is considered significant given p-values <0.05.

CRediT authorship contribution statement

Letizia Ferroni: Writing – review & editing, Visualization, Supervision, Data curation. **Andrea Rubini:** Methodology, Formal analysis. **Paolo Bargellini:** Investigation. **Elena Tremoli:** Validation. **Ilenia Pia Cappucci:** Formal analysis. **Ugo D'Amora:** Investigation. **Alfredo Ronca:** Resources, Methodology, Investigation. **Giulia Calogero:** Methodology. **Paolo Cortellini Panini:** Methodology. **Gisella Bettini:** Methodology. **Cristiana Piccoli:** Methodology. **Giuseppe Rubini:** Methodology. **Lucia Sileo:** Methodology. **Maria Pia Cavaleri:** Resources. **Luca Lovatti:** Writing – original draft, Visualization, Supervision, Data curation. **Barbara Zavan:** Writing – review & editing, Writing – original draft, Visualization, Validation, Supervision, Project administration, Methodology, Investigation, Funding acquisition, Formal analysis, Data curation, Conceptualization.

Declaration of competing interest

The authors declare that they have no known competing financial interests or personal relationships that could have appeared to influence the work reported in this paper.

Data availability

Data will be made available on request.

List of abbreviations

ADEVs – Apple-derived extracellular vesicles
cASCs – canine Adipose derived stem cells
ANOVA - Analysis of Variance
BSA – Bovine Serum Albumin
BSM - Bifidus Selective Medium
CALPRO - Calprotectin
CIBDAI - Clinical Inflammatory Bowel Disease Activity Index
EV – Extracellular Vesicles
FDR - False Discovery Rate
FOS - Fructooligosaccharides
IBD – Inflammatory Bowel Disease
LPS - Lipopolysaccharides
MBC - Minimum Bactericidal Concentration
MIC - Minimum Inhibitory Concentration
M.O. - Microorganism
MRS - Man–Rogosa–Sharpe
MRSA - Methicillin-Resistant S. Aureus
PBS – Phosphate Buffer Saline
PDEVs - Plant-derived Extracellular Vesicles
SE - Standard Error
sIgA - Secretory IgA

TEM - Transmission Electron Microscopy
TRPS – Tuneable Resistive Pulse Sensing
TSB - Tryptic Soy Broth
RT - Room Temperature
WSAVA - World Small Animal Veterinary Association

References

An, J.-H., Li, Q., Bhang, D.-H., Song, W.-J., & Youn, H.-Y. (2020). TNF-α and INF-γ primed canine stem cell-derived extracellular vesicles alleviate experimental murine colitis. *Scientific Reports, 10*, 2115.

Belkaid, Y., & Hand, T. (2014). Role of the microbiota in immunity and inflammation. *Cell, 157*, 121–141.

Bokka, R., et al. (2020). Biomanufacturing of tomato-derived nanovesicles. *Foods, 9*, 1852.

Bruno, S. P., et al. (2021). Extracellular vesicles derived from Citrus sinensis modulate inflammatory genes and tight junctions in a human model of intestinal epithelium. *Frontiers in Nutrition, 8*, Article 778998.

Cai, X., et al. (2021b). hucMSC-derived exosomes attenuate colitis by regulating macrophage pyroptosis via the miR-378a-5p/NLRP3 axis. *Stem Cell Research & Therapy, 12*, 416.

Cai, Z., Wang, S., & Li, J. (2021). Treatment of inflammatory bowel disease: A comprehensive review. *Frontiers of Medicine, 8*, Article 765474.

Cani, P. D., et al. (2008). Changes in gut microbiota control metabolic endotoxemia-induced inflammation in high-fat diet-induced obesity and diabetes in mice. *Diabetes, 57*, 1470–1481.

Cani, P. D., Hoste, S., Guiot, Y., & Delzenne, N. M. (2007). Dietary non-digestible carbohydrates promote L-cell differentiation in the proximal colon of rats. *Br J Nutr, 98*, 32–37.

Clemente, J. C., Ursell, L. K., Parfrey, L. W., & Knight, R. (2012). The impact of the gut microbiota on human health: An integrative view. *Cell, 148*, 1258–1270.

Cui, Y., Gao, J., He, Y., & Jiang, L. (2020). Plant extracellular vesicles. *Protoplasma, 257*, 3–12.

David, L. A., et al. (2014). Diet rapidly and reproducibly alters the human gut microbiome. *Nature, 505*, 559–563.

Deng, Z., et al. (2017). Broccoli-derived Nanoparticle inhibits mouse colitis by activating dendritic cell AMP-activated protein kinase. *Molecular Therapy, 25*, 1641–1654.

Díaz-Regañón, D., et al. (2023). Characterization of the fecal and mucosa-associated microbiota in dogs with chronic inflammatory enteropathy. *Animals, 13*, 326.

Fontaine, F., Turjeman, S., Callens, K., & Koren, O. (2023). The intersection of undernutrition, microbiome, and child development in the first years of life. *Nature Communications, 14*, 3554.

Gao, C., et al. (2022). Turmeric-derived nanovesicles as novel nanobiologics for targeted therapy of ulcerative colitis. *Theranostics, 12*, 5596–5614.

Glassner, K. L., Abraham, B. P., & Quigley, E. M. M. (2020). The microbiome and inflammatory bowel disease. *The Journal of Allergy and Clinical Immunology, 145*, 16–27.

Grossberg, L. B., Papamichael, K., & Cheifetz, A. S. (2022). Review article: Emerging drug therapies in inflammatory bowel disease. *Alimentary Pharmacology & Therapeutics, 55*, 789–804.

Hashimoto-Hill, S., & Alenghat, T. (2021). Inflammation-associated microbiota composition across domestic animals. *Frontiers in Genetics, 12*, Article 649599.

He, B., Hamby, R., & Jin, H. (2021). Plant extracellular vesicles: Trojan horses of cross-kingdom warfare. *FASEB Bioadv, 3*, 657–664.

Heidari, N., et al. (2021). Adipose-derived mesenchymal stem cell-secreted exosome alleviates dextran sulfate sodium-induced acute colitis by Treg cell induction and inflammatory cytokine reduction. *Journal of Cellular Physiology, 236*, 5906–5920.

Inflammatory Bowel Disease Fact Sheet. Davies Veterinary Specialists https://www.vetspecialists.co.uk/fact-sheets-post/inflammatory-bowel-disease-fact-sheet/.

Jergens, A. E., et al. (2003). A scoring Index for disease activity in canine inflammatory bowel disease. *Journal of Veterinary Internal Medicine, 17*, 291–297.

Kim, M., & Park, J. H. (2022). Isolation of aloe saponaria-derived extracellular vesicles and investigation of their potential for chronic wound healing. *Pharmaceutics, 14*, 1905.

Kopper, J. J., et al. (2021). Harnessing the biology of canine intestinal organoids to heighten understanding of inflammatory bowel disease pathogenesis and accelerate drug Discovery: A one health approach. *Front. Toxicol., 3*.

Liu, N.-J., Bao, J.-J., Wang, L.-J., & Chen, X.-Y. (2020). Arabidopsis leaf extracellular vesicles in wound-induced jasmonate accumulation. *Plant Signaling & Behavior, 15*, Article 1833142.

Liu, C., et al. (2022). Oral administration of turmeric-derived exosome-like nanovesicles with anti-inflammatory and pro-resolving bioactions for murine colitis therapy. *J Nanobiotechnology, 20*, 206.

Ma, X., et al. (2021). Lactobacillus rhamnosus and Bifidobacterium longum alleviate colitis and cognitive impairment in mice by regulating IFN-γ to IL-10 and TNF-α to IL-10 expression ratios. *Scientific Reports, 11*, Article 20659.

Malewska, K., Rychlik, A., Nieradka, R., & Kander, M. (2011). Treatment of inflammatory bowel disease (IBD) in dogs and cats. *Polish Journal of Veterinary Sciences, 14*, 165–171.

Man, F., et al. (2021). The study of ginger-derived extracellular vesicles as a natural nanoscale drug carrier and their intestinal absorption in rats. *AAPS PharmSciTech, 22*, 206.

Mayer, L. (2000). Mucosal immunity and gastrointestinal antigen processing. *Journal of Pediatric Gastroenterology and Nutrition, 30*(Suppl), S4–S12.

Nishida, A., et al. (2018). Gut microbiota in the pathogenesis of inflammatory bowel disease. *Clin J Gastroenterol, 11*, 1–10.

Pathirana, W. G. W., Chubb, S. P., Gillett, M. J., & Vasikaran, S. D. (2018). Faecal calprotectin. *Clinical Biochemist Reviews, 39*, 77–90.

Pérez-Bermúdez, P., Blesa, J., Soriano, J. M., & Marcilla, A. (2017). Extracellular vesicles in food: Experimental evidence of their secretion in grape fruits. *Eur J Pharm Sci, 98*, 40–50.

Peterson, J., et al. (2009). The NIH human microbiome Project. *Genome Research, 19*, 2317–2323.

Rhimi, S., et al. (2022). The nexus of diet, gut microbiota and inflammatory bowel diseases in dogs. *Metabolites, 12*, 1176.

Shen, Z., et al. (2021). Effects of mesenchymal stem cell-derived exosomes on autoimmune diseases. *Frontiers in Immunology, 12*, Article 749192.

Suchodolski, J. S., et al. (2012). The fecal microbiome in dogs with acute diarrhea and idiopathic inflammatory bowel disease. *PLoS One, 7*, Article e51907.

Takeuchi, T., et al. (2023). Gut microbial carbohydrate metabolism contributes to insulin resistance. *Nature, 621*, 389–395.

Trentini, M., et al. (2022a). An apple a day keeps the doctor away: Potential role of miRNA 146 on macrophages treated with exosomes derived from apples. *Biomedicines, 10*, 415.

Trentini, M., et al. (2022b). Apple derived exosomes improve collagen type I production and decrease MMPs during aging of the skin through downregulation of the NF-κB pathway as mode of action. *Cells, 11*, 3950.

Trentini, M., et al. (2024). Link between organic nanovescicles from vegetable kingdom and human cell physiology: Intracellular calcium signalling. *J Nanobiotechnology, 22*, 68.

The triple burden of malnutrition. *Nat Food, 4*, (2023), 925–925.

Valdes, A. M., Walter, J., Segal, E., & Spector, T. D. (2018). Role of the gut microbiota in nutrition and health. *BMJ, k2179*. https://doi.org/10.1136/bmj.k2179

Vázquez-Baeza, Y., Hyde, E. R., Suchodolski, J. S., & Knight, R. (2016). Dog and human inflammatory bowel disease rely on overlapping yet distinct dysbiosis networks. *Nat Microbiol, 1*, Article 16177.

Ye, L., et al. (2023). Repressed Blautia-acetate immunological axis underlies breast cancer progression promoted by chronic stress. *Nature Communications, 14*, 6160.

You, J. Y., Kang, S. J., & Rhee, W. J. (2021). Isolation of cabbage exosome-like nanovesicles and investigation of their biological activities in human cells. *Bioactive Materials, 6*, 4321–4332.